

## On the origin of the distribution of binary-star periods

Pavel Kroupa<sup>1</sup> and Andreas Burkert<sup>2</sup>

<sup>1</sup> Institut für Theoretische Physik und Astrophysik  
Universität Kiel, D-24098 Kiel, Germany

<sup>2</sup>Max-Planck-Institut für Astronomie, Königstuhl 17  
D-69117 Heidelberg, Germany

### Summary

Pre-main sequence and main-sequence binary systems are observed to have periods,  $P$ , ranging from one day to  $10^{10}$  days and eccentricities,  $e$ , ranging from 0 to 1. We pose the problem if stellar-dynamical interactions in very young and compact star clusters may broaden an initially narrow period distribution to the observed width.  $N$ -body computations of extremely compact clusters containing 100 and 1000 stars initially in equilibrium and in cold collapse are preformed. In all cases the assumed initial period distribution is uniform in the narrow range  $4.5 \leq \log_{10} P \leq 5.5$  ( $P$  in days) which straddles the maximum in the observed period distribution of late-type Galactic-field dwarf systems. None of the models lead to the necessary broadening of the period distribution, despite our adopted extreme conditions that favour binary–binary interactions. Stellar-dynamical interactions in embedded clusters thus cannot, *under any circumstances*, widen the period distribution sufficiently. The wide range of orbital periods of very young and old binary systems is therefore a result of cloud fragmentation and immediate subsequent magneto-hydrodynamical processes operating within the multiple proto-stellar system.

*Subject headings:* binaries: general – stars: formation – stars: late-type – open clusters and associations: general – methods: n-body simulations

### 1. INTRODUCTION

The distribution of orbital parameters of binary systems pose important constraints on the theory of star-formation. In particular, the distribution of eccentricities and periods of late-type Galactic-field binary systems are sufficiently well observed to address the issue of their origin.

The observed eccentricity distribution is approximately thermal ( $f_e \sim 2e$ , with  $f_e de$  being the number of orbits in the interval  $e$  to  $e+de$ ) for binaries with periods  $P \gtrsim 10^3$  days, but for systems with  $P \lesssim 10^3$  days,  $e$  and  $P$  are correlated such that smaller  $P$  imply, on average, smaller  $e$ . For Galactic late-type dwarfs the distribution of periods,  $f_P$ , is log-normal in  $P$ , with the notable feature that  $P$  ranges from 1 to  $10^{10}$  days

---

<sup>1</sup>pavel@astrophysik.uni-kiel.de

<sup>2</sup>burkert@mpia-hd.mpg.de

with a mean  $\log_{10}P \approx 4.8$  (fig. 1 in Kroupa 1995a). Pre-main sequence binaries show the same wide range of parameters and correlations (Mathieu 1994).

The available cloud-collapse calculations have not been able to produce the wide range of observed periods, and in particular do not lead to short-period ( $P \lesssim 10^3$  d) systems (Bodenheimer et al. 2000 for a review). However, even the most recent numerical refinements cannot describe stellar formation to the point where gas-dynamical processes can be neglected, so that the final theoretical orbital parameters of binary systems cannot be quantified. We do not know for sure yet if there exists some significant magneto-hydrodynamical mechanism that is important in transforming a theoretical period distribution that results from fragmentation to the final wide  $f_P$  observed already among 1 Myr old populations. Alternatively, it may be possible that no such mechanism is needed, and that the final (observed) orbital parameters of Galactic-field systems are a result of gravitational encounters in very dense embedded clusters that disperse rapidly.

It has already been demonstrated that stellar-dynamical interactions in typical embedded clusters spanning a wide range of densities cannot significantly widen a period distribution. Too few orbits are redistributed to  $P < 10^3$  days by encounters assuming the primordial period distribution is confined to the range  $10^3 - 10^{7.5}$  days. Similarly, typical embedded clusters cannot evolve an arbitrary eccentricity distribution to the thermal form (Kroupa 1995b).

The purpose of the present paper is to study the evolution of a range of *extremely dense* clusters to answer the question once and for all whether encounters within a dense cluster environment can significantly contribute to the observed width of  $f_P$ . Section 2 briefly describes the codes used for the  $N$ -body computations and the data reduction, and the initial conditions. The results are presented in Section 3, and the conclusions follow in Section 4.

## 2. THE CODES AND INITIAL CONDITIONS

### 2.1. The $N$ -body programme

A direct  $N$ -body code must deal efficiently with a range of dynamical time-scales spanning many orders of magnitude, from days to hundreds of Myrs. The code of choice is Aarseth’s NBODY6 (Aarseth 1999). Special mathematical techniques are employed to transform the space-time coordinates of closely interacting stars, which may be perturbed by neighbours, such that the resulting equations of motion of the sub-system are regular (Mikkola & Aarseth 1993). State-of-the-art stellar evolution is incorporated (Hurley, Pols & Tout 2000), as well as a standard Galactic tidal field (Terlevich 1987).

The velocity and position vectors of any individual centre-of-mass particle (e.g. a star or binary system) diverges exponentially from the true trajectory, through the growth of errors in  $N$ -body computations (e.g. Goodman, Heggie & Hut 1993). However, statistical results from  $N$ -body calculations correctly describe the overall dynamical evolution, as shown, for example, by Giersz & Heggie (1994) who compare ensembles of  $N$ -body computations with statistical stellar-dynamical methods. Thus, for each model constructed here an ensemble is created in order to obtain reliable estimates of the relevant statistical quantities.

The output from NBODY6 is analysed by a software package that finds all bound binary systems, and allows the construction of distribution functions of orbital parameters, among many other things.

## 2.2. Initial binary systems

Initial stellar masses are distributed according to a three-part power-law IMF (Kroupa 2001b),  $\xi(m) \propto m^{-\alpha}$ , where  $\alpha = 0.3$  for  $0.01 \leq m < 0.08 M_{\odot}$ ,  $\alpha = 1.3$  for  $0.08 \leq m < 0.5 M_{\odot}$  and  $\alpha = 2.3$  for  $0.5 \leq m/M_{\odot}$ , and  $\xi(m) dm$  is the number of stars in the mass range  $m$  to  $m + dm$ .

The total binary proportion is

$$f_{\text{tot}} = \frac{N_{\text{bin}}}{N_{\text{bin}} + N_{\text{sing}}}, \quad (1)$$

where  $N_{\text{bin}}$  and  $N_{\text{sing}}$  are the number of binary and single-star systems, respectively. Initially, all stars are assumed to be in binary systems ( $f_{\text{tot}} = 1$ ) with component masses  $m_1, m_2$  chosen randomly from the IMF.

The initial logarithmic binary-star periods are distributed uniformly in the narrow interval  $4.5 \leq \log_{10} P \leq 5.5$ ,  $P$  in days. The period distribution of late-type systems is

$$f_P = \frac{N_{\text{bin,P,lt}}}{N_{\text{bin,lt}} + N_{\text{sing,lt}}}, \quad (2)$$

where  $N_{\text{bin,P,lt}}$  is the number of binaries with orbits in the interval  $\log_{10} P$  and  $\log_{10} P + d\log_{10} P$  in which the primary has a mass  $0.08 \leq m \leq 1.5 M_{\odot}$ , and  $N_{\text{sing,lt}}, N_{\text{bin,lt}}$  are the number of single stars and binaries with primaries, respectively, in this mass interval. The initial ( $t = 0$ ) period distribution is given by

$$f_P = \begin{cases} 0.5 & : 4.5 \leq \log_{10} P \leq 5.5, \\ 0.0 & : \text{otherwise,} \end{cases} \quad (3)$$

the period distribution being constructed using decade intervals in  $P$  (see Fig. 4 below). All binary systems initially have orbits with eccentricity  $e = 0.75$ , but the results are not sensitive to this value (Kroupa 1995b).

These assumptions allow us to test the hypothesis that binary–binary and binary–single-star encounters in very compact young clusters widen the period distribution to the form observed in the Galactic field, and re-distribute the eccentricities to give the thermal distribution observed for Galactic-field systems.

## 2.3. Cluster models

Clusters initially in virial equilibrium (VE) and in cold collapse (CC) with  $N = 100$  and 1000 stars are set up to cover a range of extreme initial conditions (Table 1).

The VE models are spherical Plummer number-density profiles (Aarseth, Hénon & Wielen 1974) initially, with position and velocity vectors not correlated with the system masses. The initial half-mass radius,  $R_{0.5}$ , is chosen to give a three-dimensional velocity dispersion,  $\sigma_{3D}$ , that equals the orbital velocity of a binary with a system mass of  $1 M_{\odot}$  and a period,  $P = 10^5$  days, near the maximum in the G-dwarf period distribution of Duquennoy & Mayor (1991). The central densities of these models are extreme and probably unrealistic, in that many of the binary systems overlap. However, these models allow us to study the very extreme situation in which binary–binary interactions dominate initial cluster evolution, and will thus pose limits on the possible widening of the period distribution as a result of these interactions.

The CC models are uniform spheres, each cluster having no initial velocity dispersion, with the position vectors and system masses being uncorrelated. The increased binary–binary interactions near maximum collapse may widen the period distribution to the observed values.

### 3. RESULTS

#### 3.1. Cluster evolution

The evolution of the clusters is exemplified by evaluating the core radius,  $R_C(t)$  (e.g. Kroupa, Aarseth & Hurley 2001). This quantity measures the degree of concentration of a cluster. The central number density is the density within  $R_C$ , counting all stars and brown dwarfs. The evolution of both quantities is shown in Fig. 1.

The core radius of the VE models increases immediately as a consequence of binary-star heating for the highly concentrated N2v and N2v1 models, whereas it decreases in the less concentrated N3v model during the first few  $t_{cr}$  as a result of mass segregation. When energy re-arrangement through mass segregation has ended, the most massive stars having reached the centre,  $R_C$  also expands in this model. It is interesting to note that the increase follows a power-law,  $R_C \propto t^{r_R}$  with  $r_R \approx 0.95$ , in all cases. The central density decreases as a power-law,  $\rho_C \propto t^{r_\rho}$  with  $r_\rho \approx -2.2$ . The decay in  $\rho_C$  sets-in immediately in models N2v and N2v1, but is retarded in model N3v as a result of the settling of the heavy stars.

The CC models contract homologously until local density fluctuations have increased sufficiently to form one dominating potential well, thus focusing the further radial flow (Aarseth, Lin & Papaloizou 1988). At this point  $\rho_C$  begins to increase until it reaches a maximum which defines the time of maximum contraction,  $R_C$  being smallest then. After violent relaxation the compactified clusters evolve as the VE models, albeit with a time-lag through the collapse.

The clusters can be taken to be dissolved when  $\rho_C \lesssim 5$  stars/pc<sup>3</sup>. The ‘final’ distributions of orbital parameters discussed below are evaluated approximately at this time taking account of all stars, when no further stellar-dynamical, or stimulated, evolution of the binary population occurs.

#### 3.2. The binaries

The evolution of  $f_{tot}$  is plotted for all models in Fig. 2.

As noted above, the binaries initially overlap in the VE models, causing immediate disruption of the widest systems leading to a population of single stars in the cluster. Further binary depletion occurs on a crossing time-scale. Meanwhile the cluster expands (Fig. 1), slowing further binary disruption, until it is virtually halted at the point when the remaining binary population is hard in the expanded cluster (Kroupa 2001a). Fig. 2 shows that finally  $f_{tot} \approx 0.2$  for models N2v/v1, and  $f_{tot} \approx 0.4$  for model N3v. These values are too low in comparison with the Galactic field ( $f_{tot}^{obs} \approx 0.6$ ), let alone with pre-main sequence binaries ( $f_{tot}^{obs} \approx 0.8 - 1$ ).

In the CC models, binary disruption starts as soon as the cluster has contracted sufficiently for the widest pairs to interact. Disruption continues throughout and beyond cold collapse, with binaries with an increasing binding energy playing an increasing role. During this time, an increasing amount of kinetic energy is used up to disrupt these binaries. How the cold collapse is affected by such a large primordial binary population is an interesting topic, but will not be addressed further here. In both CC models, the final  $f_{tot}$  is slightly higher than the binary proportion in the Galactic field.

During the binary–binary interactions some systems are perturbed or exchange companions, rather

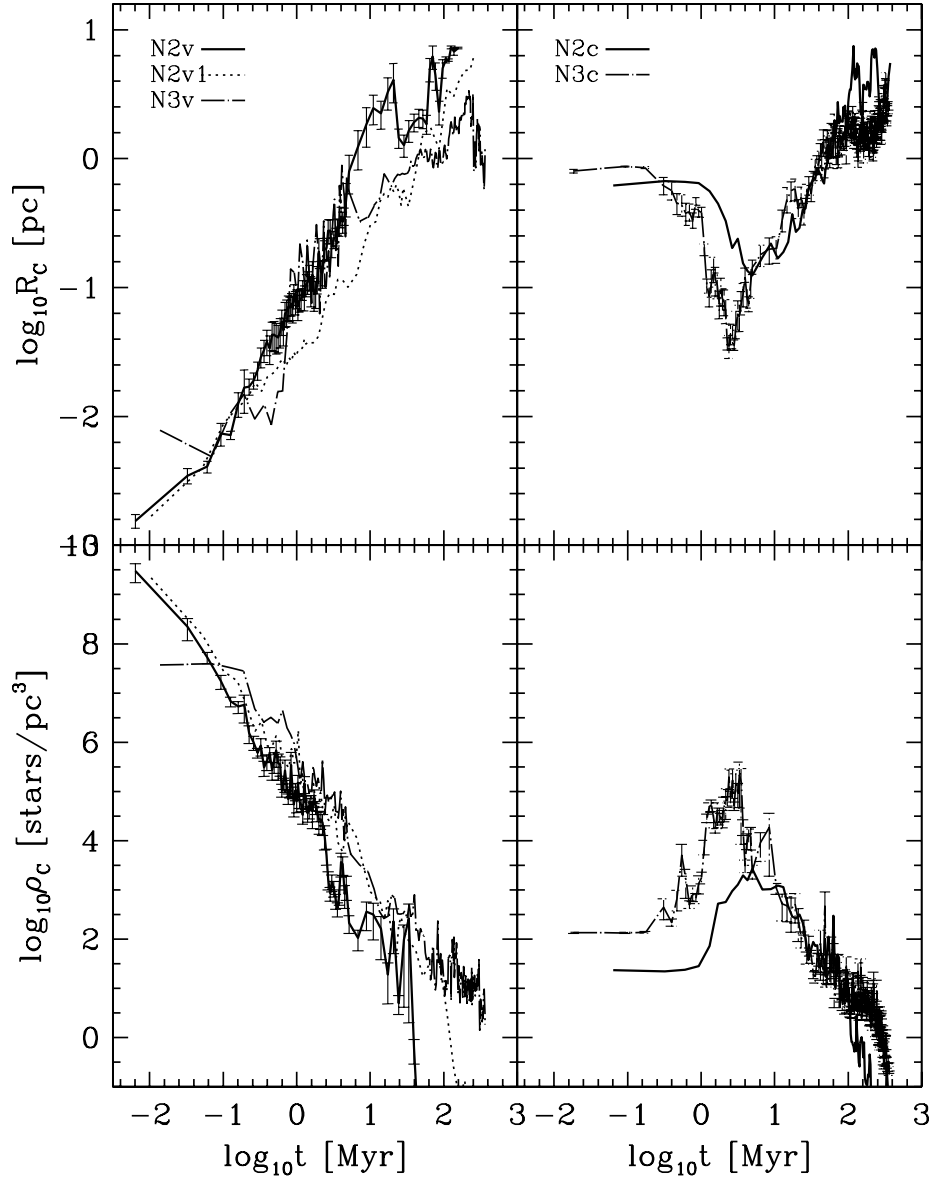


Fig. 1.— The core radius and central density. The scales are identical in the top two and lower two panels. For clarity, the standard error of the mean is shown for one model in each panel.

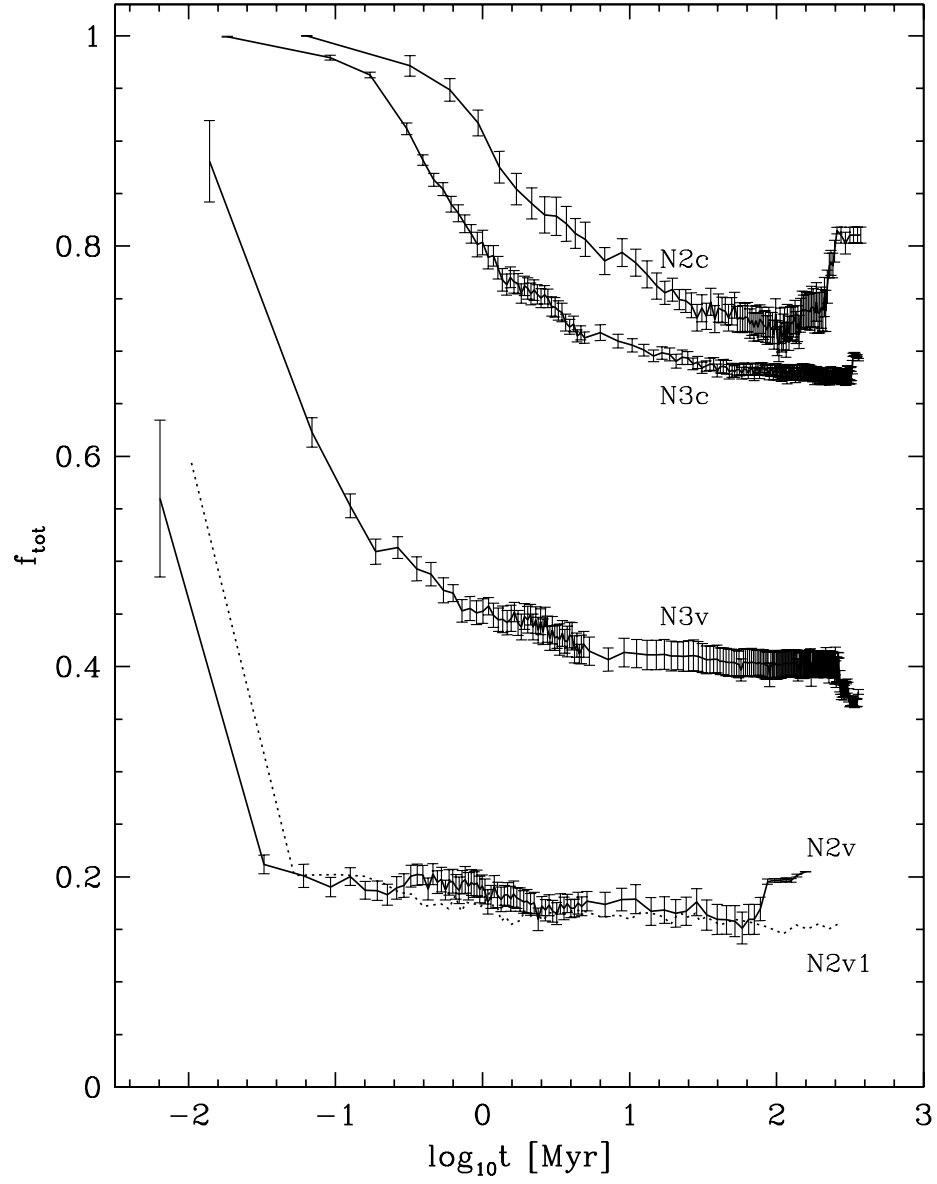


Fig. 2.— The evolution of the binary proportion (eqn 1). Error-bars are standard error of the mean.

than being disrupted. This leads to changes in their orbital parameters. The final distributions of orbits in the eccentricity–period diagram are shown in Fig. 3.

A significant broadening of the eccentricity distribution is evident, but the final distributions retain a maximum near  $e = 0.75$  which is not consistent with the observational distribution (Duquennoy & Mayor 1991). Thus, the stellar-dynamical encounters in extremely concentrated clusters cannot evolve a delta-eccentricity distribution to the observed thermal distribution.

Similarly, a significant but not sufficient broadening of the period distribution,  $f_P$ , occurs in models N2v/v1, but the effect on  $f_P$  is small in the other models. Fig. 4 demonstrates that the initial distribution cannot evolve through stellar-dynamical interactions to the observed broad log-normal distribution. This is the case even under the extreme assumption that the evolution of the N2v1 cluster is halted pre-maturely, for example through the expulsion of the remnant natal gas, and that the single-star population that emerges from the disruption of the binaries is lost preferentially through ejection and mass segregation before gas-expulsion. In this thought experiment,  $f_P$  will appear enhanced, since  $f_P = \eta N_{\text{bin,P,lt}}$  with  $\eta = (N_{\text{bin,lt}} + N_{\text{sing,lt}})^{-1}$  (eqn 2). In Fig. 4,  $f'_P = 3 \times f_P$  is plotted for model N2v1, but even this artificially enhanced period distribution disagrees with the observed distribution.

#### 4. CONCLUSION

The finding is thus that stellar-dynamical interactions in compact star clusters cannot change an initially delta-eccentricity distribution and narrow period distribution to the thermal eccentricity and wide log-period distribution observed in the Galactic field. It follows that the main characteristics of these distributions (thermal  $f_e$  and orbits ranging from days to Myrs) must be a result of fragmentation during star-formation and subsequent magneto-hydrodynamical processes.

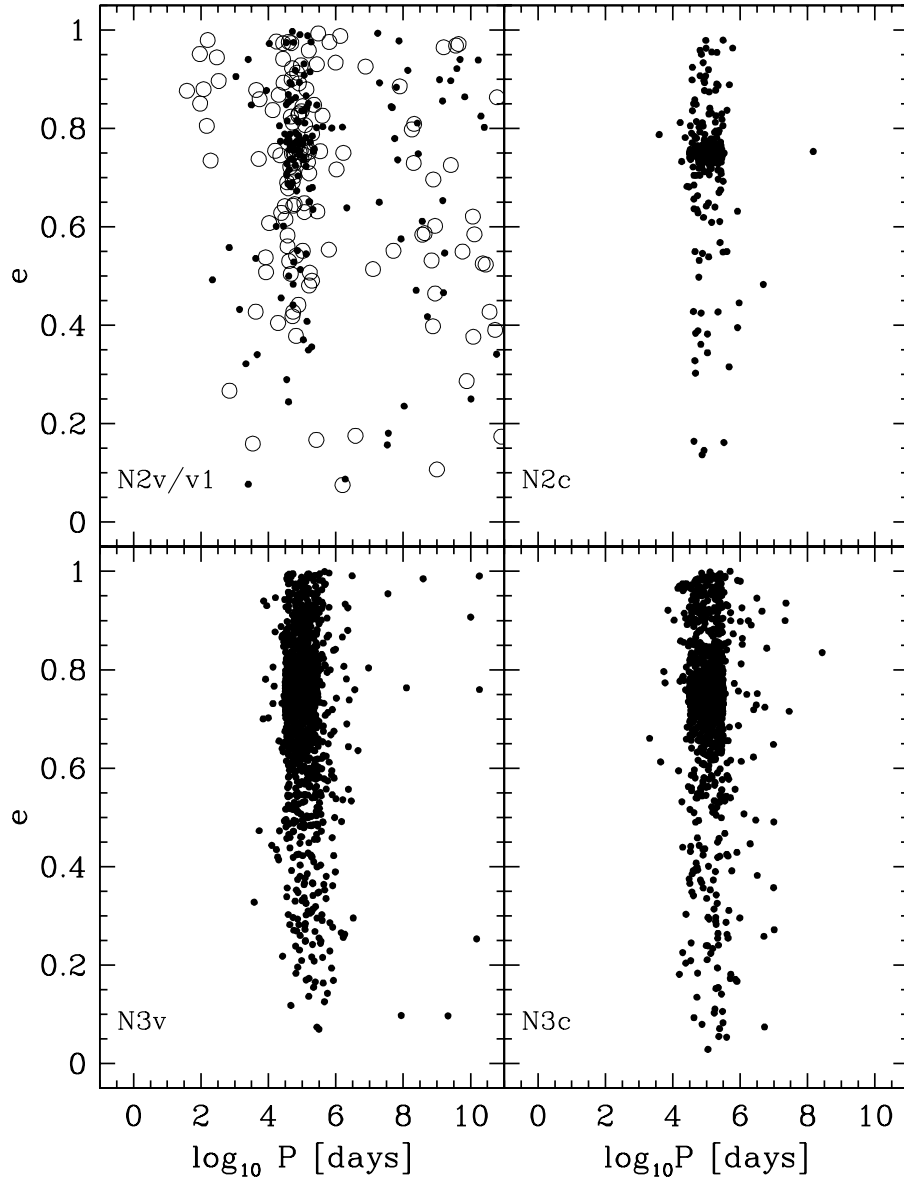


Fig. 3.— The final distributions in the eccentricity–period diagram. The solid and open circles in the upper left panel are for model N2v and N2v1, respectively. The initial ( $t = 0$ ) distribution is given by  $e = 0.75$  and  $10^{4.5} \leq P \leq 10^{5.5}$ .



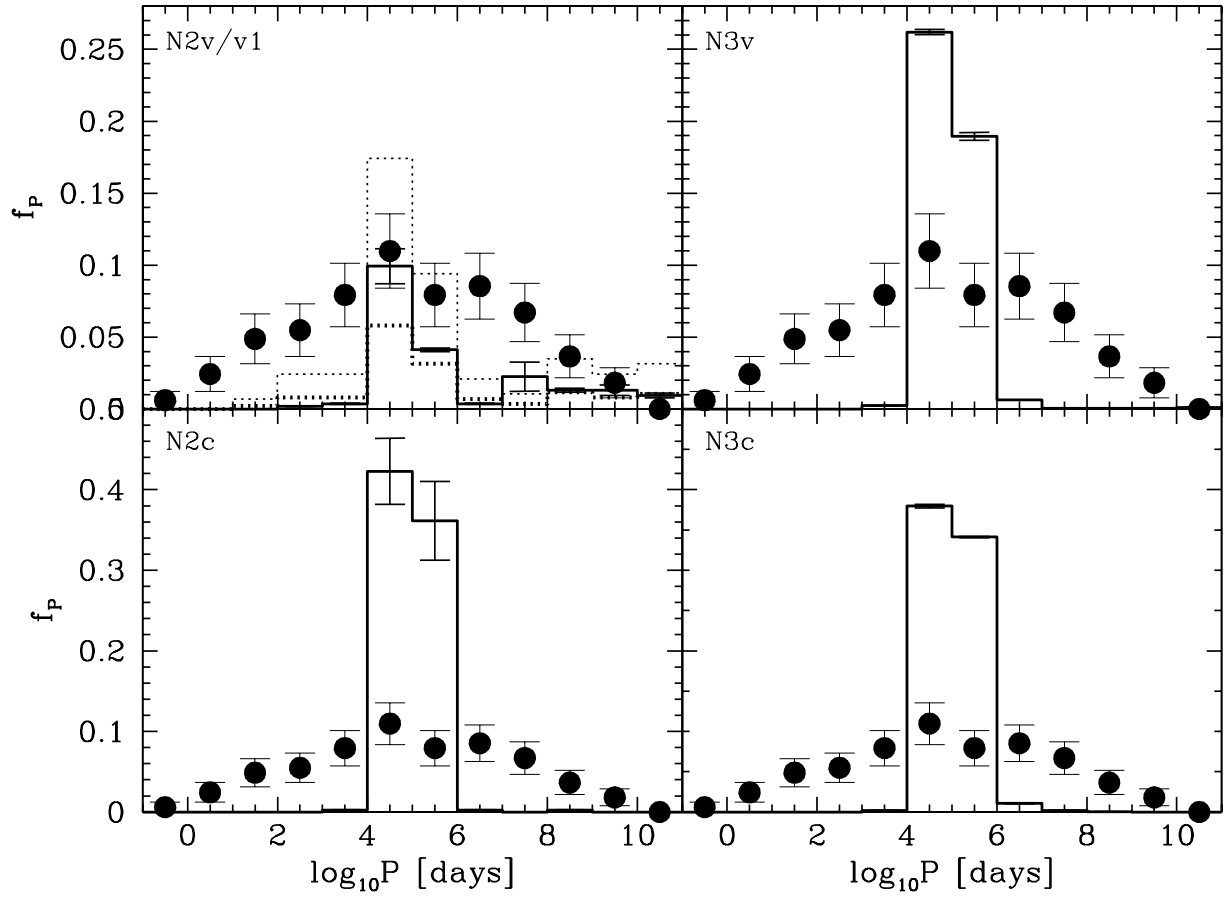


Fig. 4.— The final period distributions. For model N2v1,  $f_P$  and  $3 \times f_P$  are plotted as thick and thin dotted lines, respectively (see text). The initial distributions are given by eqn. 3. Filled circles show the G-dwarf period distribution from Duquennoy & Mayor (1992). M and K dwarfs have indistinguishable distributions (e.g. fig. 1 in Kroupa 1995a).

## Acknowledgements

The  $N$ -body calculations were performed on computers at the Institute for Theoretical Astrophysics, Heidelberg University, using a variant of Aarseth's NBODY6 code.

## REFERENCES

- Aarseth S.J., 1999, *PASP*, 111, 1333
- Aarseth S.J., Hénon M., Wielen R., 1974, *A&A*, 37, 183
- Aarseth S.J., Lin D.N.C, Papaloizou J.C.B., 1988, *ApJ*, 324, 288
- Bodenheimer P., Burkert A., Klein R.I., Boss A.P., 2000, in *Protostars and Planets IV*, eds. V. Mannings, A.P. Boss & S.S. Russell, University of Arizona Press, Tucson, p.675
- Duquennoy A., Mayor M., 1991, *A&A*, 248, 485
- Giersz M., Heggie D.C., 1994, *MNRAS*, 268, 257
- Goodman J., Heggie D.C., Hut P., 1993, *ApJ*, 415, 715
- Hurley J.R., Pols O.R., Tout C.A., 2000, *MNRAS*, 315, 543
- Kroupa P., 1995a, *MNRAS*, 277, 1491
- Kroupa P., 1995b, *MNRAS*, 277, 1507
- Kroupa P., 2001a, in *The Formation of Binary Stars*, IAU Symp. 200, eds. H. Zinnecker & R. Mathieu, ASP Conf. Ser., in press (astro-ph/0010347)
- Kroupa P., 2001b, *MNRAS*, in press (astro-ph/0009005)
- Kroupa P., Aarseth S.J., Hurley J.R., 2001, *MNRAS*, in press (astro-ph/0009470)
- Mathieu R.D., 1994, *ARA&A*, 32, 465
- Mikkola S., Aarseth S.J., 1993, *Cel. Mech. Dyn. Astron.*, 57, 439
- Terlevich E., 1987, *MNRAS*, 224, 193

model	$N$	$R_{0.5}$	$\langle m \rangle$	$\sigma_{3D}$	$\log_{10} t_{cr}$	$\log_{10} \rho_C$	$M_{cl}$	$N_{run}$	Dynamical state
		[pc]	$[M_\odot]$	[km/s]	[Myr]	[stars/pc <sup>3</sup> ]	$[M_\odot]$		
N2v	$10^2$	0.00287	0.37	4.59	−2.90	9.4	37	10	VE
N2v1	$10^2$	0.0040	0.30	3.87	−2.68	8.9	30	10	VE
N3v	$10^3$	0.0287	0.37	4.59	−1.90	7.4	370	5	VE
N2c	$10^2$	1.2	0.37	0.0	+0.69	1.1	37	10	CC
N3c	$10^3$	1.2	0.37	0.0	+0.37	2.1	37	5	CC

Table 1: Initial cluster models.  $N$  is the total number of stars, and  $M_{cl}$  the cluster mass.  $R_{0.5}$  is the half-mass radius of the Plummer-density distribution for the models that are initially in virial equilibrium (VE). It is the radius of the homogenous sphere for the models that undergo cold collapse (CC) that have a vanishing initial three-dimensional velocity dispersion  $\sigma_{3D}$ . The central density is  $\rho_C$ . All models, except N2v1, have stars in the mass range  $0.01 - 50 M_\odot$  giving a mean stellar mass  $\langle m \rangle = 0.37 M_\odot$ . Model N2v1 contains only stars with  $0.08 \leq m \leq 1.1 M_\odot$  having  $\langle m \rangle = 0.30 M_\odot$ . It contains no brown dwarfs and massive stars, and thus provides comparison data for the more realistic other cases. No significant differences emerge. In the VE models,  $t_{cr}$  is the crossing time, whereas it is the time until maximum contraction in the CC models. Each model is computed  $N_{run}$  times, each with a different random number seed.